Arteriosclerosis, Thrombosis, and Vascular Biology

TRANSLATIONAL SCIENCES

Variation in Coronary Atherosclerosis Severity Related to a Distinct LDL (Low-Density Lipoprotein) Profile

Findings From a Familial Hypercholesterolemia Pig Model

Ayla Hoogendoorn, Sandra den Hoedt, Eline M.J. Hartman, Ilona Krabbendam-Peters, Maaike te Lintel Hekkert, Leonie van der Zee, Kim van Gaalen, Karen Th. Witberg, Kristien Dorst, Jurgen M.R. Ligthart, Ludovic Drouet, Kim Van der Heiden, Jeanine Roeters van Lennep, Antonius F.W. van der Steen, Dirk J. Duncker, Monique T. Mulder, Jolanda J. Wentzel

OBJECTIVE: In an adult porcine model of familial hypercholesterolemia (FH), coronary plaque development was characterized. To elucidate the underlying mechanisms of the observed inter-individual variation in disease severity, detailed lipoprotein profiles were determined.

APPROACH AND RESULTS: FH pigs (3 years old, homozygous *LDLR* R84C mutation) received an atherogenic diet for 12 months. Coronary atherosclerosis development was monitored using serial invasive imaging and histology. A pronounced difference was observed between mildly diseased pigs which exclusively developed early lesions (maximal plaque burden, 25% [23%–34%]; n=5) and advanced-diseased pigs (n=5) which developed human-like, lumen intruding plaques (maximal plaque burden, 69% [57%–77%]) with large necrotic cores, intraplaque hemorrhage, and calcifications. Advanced-diseased pigs and mildly diseased pigs displayed no differences in conventional risk factors. Additional plasma lipoprotein profiling by size-exclusion chromatography revealed 2 different LDL (low-density lipoprotein) subtypes: regular and larger LDL. Cholesterol, sphingosine-1-phosphate, ceramide, and sphingomyelin levels were determined in these LDL-subfractions using standard laboratory techniques and high-pressure liquid chromatography mass-spectrometry analyses, respectively. At 3 months of diet, regular LDL of advanced-diseased pigs contained relatively more cholesterol (LDL-C; regular/larger LDL-C ratio 1.7 [1.3–1.9] versus 0.8 [0.6–0.9]; P=0.008) than mildly diseased pigs, while larger LDL contained more sphingosine-1-phosphate, ceramides, and sphingomyelins. Larger and regular LDL was also found in plasma of 3 patients with homozygous FH with varying LDL-C ratios.

CONCLUSIONS: In our adult FH pig model, inter-individual differences in atherosclerotic disease severity were directly related to the distribution of cholesterol and sphingolipids over a distinct LDL profile with regular and larger LDL shortly after the diet start. A similar LDL profile was detected in patients with homozygous FH.

VISUAL OVERVIEW: An online visual overview is available for this article.

Key Words: animal model ■ atherosclerosis ■ biomarker ■ coronary artery disease ■ familial hypercholesterolemia ■ hypercholesterolemia ■ sphingolipids

Downloaded from http://ahajournals.org by on November 7, 2019

Coronary atherosclerotic plaque destabilization and rupture is one of the most important causes of acute coronary events and sudden death.[1–3] Therefore, risk-assessment of atherosclerotic plaques before the occurrence of an acute coronary event is an important focus of coronary artery disease (CAD) research. Herein, in vivo

Correspondence to: Monique T. Mulder, PhD, PO Box 2040, 3000 CA Rotterdam, the Netherlands, Email m.t.mulder@erasmusmc.nl; or Jolanda J. Wentzel, PhD, PO Box 2040, 3000 CA Rotterdam, the Netherlands. Email j.wentzel@erasmusmc.nl

The online-only Data Supplement is available with this article at https://www.ahajournals.org/doi/suppl/10.1161/ATVBAHA.119.313246.

For Sources of Funding and Disclosures, see page 2351.

© 2019 The Authors. *Arteriosclerosis, Thrombosis, and Vascular Biology* is published on behalf of the American Heart Association, Inc., by Wolters Kluwer Health, Inc. This is an open access article under the terms of the Creative Commons Attribution Non-Commercial-NoDerivs License, which permits use, distribution, and reproduction in any medium, provided that the original work is properly cited, the use is noncommercial, and no modifications or adaptations are made.

Arterioscler Thromb Vasc Biol is available at www.ahajournals.org/journal/atvb

Nonstandard Abbreviations and Acronyms

AD	advanced-diseased pig
Cer	ceramide
DGUC	density-gradient ultracentrifuge
FCA	fibrous cap atheroma
FH	familial hypercholesterolemia
FPLC	fast-protein liquid chromatography
HDL	high-density lipoprotein
HDL-C	HDL-cholesterol
IVUS	intravascular ultrasound
LDL	low-density lipoprotein
LDL-C	LDL-cholesterol
MD	mildly diseased pig
OCT	optical coherence tomography
S1P	sphingosine-1-phosphate
SM	sphingomyelin
VLDL	very-low-density lipoprotein

Highlights

- Adult familial hypercholesterolemia pigs on an atherogenic diet developed coronary atherosclerosis with a clear distinction between mildly diseased pigs and advanced-diseased pigs.
- Plaques in the advanced-diseased pigs progressed to lumen intruding human-like plaques with vulnerable characteristics including lipid-rich necrotic cores, calcifications, neovascularization, and intraplaque hemorrhage.
- The observed inter-individual differences in atherosclerotic disease severity in the pigs were directly related to the distribution of cholesterol and sphingolipids over a distinct LDL profile with regular and larger LDL observed shortly after the start of the diet.
- A similar LDL profile was detected in homozygous patients with FH, a finding that holds promise for early individual cardiovascular disease detection, but also as a treatment target.

studies with serial imaging and histopathological analyses are essential to understand the mechanisms and causative factors of plaque growth and destabilization. Unfortunately, natural history studies in humans are limited by the long time-frame of disease development, by the small number of longitudinal (invasive) imaging time points, and by the very limited possibility to collect tissue. This urges the need for a preclinical animal model that presents with human-like CAD.

See accompanying editorial on page 2203
See cover image

Because of their comparable coronary size, anatomy and diet, pigs are currently the animal model that most closely resembles the human disease pathophysiology, and that is most suitable for testing new imaging methods.[4–6] Atherosclerosis development in pig models is often stimulated by an atherogenic diet[7] or diabetes mellitus, or a combination of them.[8–14] Some of the most successful porcine models for nonsurgical induced atherosclerosis carry mutations in genes that regulate the lipid metabolism, like in the *LDLR*[15,16] or *PCSK9*[17] genes. These mutations are similar to those found in patients with familial hypercholesterolemia (FH) and result in high plasma cholesterol levels.[18] On an atherogenic diet, these FH pig models do develop (coronary) atherosclerotic disease, but, like in most other pig models, plaque progression is often modest, and does not reach human-like advanced disease stages with symptomatic plaques, especially in the coronary arteries.

Previous studies with atherosclerotic pig models assessed plaque development exclusively in young, growing animals. For humans, it is known that lipid profiles, blood pressure, arterial mechanics, and inflammatory status are very different between adolescents and older people,[19–21] while these are factors with a major impact on atherosclerotic disease development. These factors may thus also affect atherosclerosis development in young pigs. Therefore, we refined a previously described and promising *LDLR* mutation mini-pig model[15] by using adult animals from the start of the study. Furthermore, in contrast to earlier studies, we followed these animals for up to one year after the start of an atherogenic diet and monitored natural atherosclerotic plaque development and composition in the coronary arteries using multiple invasive imaging techniques and histology. We provide a detailed analysis on plaque size, localization, and composition at 3 time points during the follow-up period on atherogenic diet as a road-map for future studies with this promising pig model. To unravel the underlying mechanisms contributing to the observed inter-individual variation in coronary atherosclerotic plaque development that is observed similarly in patients with FH,[22] we deployed a detailed plasma lipoprotein analysis.

MATERIALS AND METHODS

Please see Methods and the Major Resources Table in the online-only Data Supplement for further details on the histological staining methods and analysis, on the invasive image analysis, and on the lipoprotein profiling methods.

Pig Model, Plaque Imaging, and Histology

The animal study protocol was approved by the local animal ethics committee (DEC EMC3318 [109-14-10]), and the study was performed according to the National Institutes of Health guide for the Care and Use of Laboratory animals.[23] FH Bretonchelles Meishan minipigs homozygous for the *LDLR* R84C mutation (FBM, n=11, castrated male) as described before by Thim et al,[15] were fed a normal laboratory diet (No. 102243/60, Sanders Ouest, Etrelles, France) until the start of

Downloaded from http://ahajournals.org by on November 7, 2019

the study. Since female pigs of this breed develop considerably less coronary atherosclerosis (unpublished data by Drouet et al), and since the main aim of this study was to study development of advanced atherosclerosis in this pig model, only castrated males were used. At the age of 34±3 months, an atherogenic diet (10% lard and 0.75% cholesterol, The National Institute of Agronomic Research, France) was started. Plaque development in the coronary arteries was monitored by performing invasive imaging of the left anterior descending, the left circumflex, and the right coronary artery using intravascular ultrasound (IVUS) and optical coherence tomography (OCT). The imaging protocol was performed at 3 time points (3 [T_1], 9 [T_2], and 10 to 12 [T_3] months on atherogenic diet) to assess (changes in) plaque size and composition.

The day before the imaging procedure, the pigs were fasted and were given an oral loading dose of 300 mg carbasalate calcium. On the day of the procedure, the animals were sedated with a mix of Xylazine (2.25 mg/kg, 20 mg/mL) and Zoletil 100 (tiletamine/zolazepam; 6 mg/kg, 100 mg/mL) injected intramuscularly, anesthetized with sodium thiopental (4 mg/kg, 50 mg/mL) administered via an ear vein, intubated and ventilated with oxygen (25%–30% v/v) and nitrogen (75%–80% v/v) to maintain blood gases within the physiological range. Anesthesia was maintained by isoflurane inhalation (1%–2.5% v/v).

Via a carotid sheath, arterial blood samples were collected, and 250 mg acetylsalicylic acid and 10 000 units of heparin were administered to prevent blood clotting. Heparin administration was repeated every hour in a dose of 5000 units. Subsequently, a guiding catheter (Mach 1, 8F, various types, Boston Scientific, Marlborough, MA) was advanced through the carotid sheath into the ostium of either one of the 3 main coronary arteries under angiographic guidance to perform a series of imaging procedures. Before imaging, isosorbide mononitrate (0.04 mg/kg, 1 mg/mL) was administered via the guiding catheter to induce epicardial coronary vasodilation. Starting position of all imaging catheters was registered by serial monoplane angiography under at least 2 angles. First, an OCT catheter (Dragonfly Optis Imaging Catheter, St Jude Medical, St Paul, MN) was advanced into the artery as distal as possible up to a maximal depth of 75 mm. A pullback of 75 mm (36 mm/s) was performed under a constant contrast (Visipaque 320, GE Healthcare, Buckinghamshire, United Kingdom) flush rate of 4 mL/s (Medrad Injection System, Bayer HealthCare LLC, Whippany, NJ). Subsequently, an IVUS catheter (TVC Insight Coronary Imaging Catheter, InfraRedX, Burlington, MA) was positioned at the same anatomic location as the OCT catheter, and a pullback (0.5 mm/s) was performed. During the IVUS pullback, the heart rate was closely monitored and registered for later use in IVUS triggering.

During the imaging procedure at the first time point, one of the pigs died due to an acute cardiac tamponade and was excluded from the study. Furthermore, fast plaque development in 2 other pigs led to cardiovascular complications and subsequent early sacrifice shortly after T_2. Of these 2 latter pigs, the data of T_1 and T_2 were used for analysis. After the final imaging time point, the pigs were euthanized, and the coronary arteries were collected for histology.

Coronary tissue was sampled every 3 mm and was used for histological (Hematoxylin and Eosin, Resorcin-Fuchsin or Miller [collagen and elastin], Oil-red-O [lipids] and Martius, Scarlet and Blue [fibrin]) and immunohistochemical stainings (CD68 [macrophages], CD31 [endothelial cells]). For the analysis, histological slides taken every 3 mm were classified according to the revised AHA classification[24] as no plaque, intimal thickening (IT), intimal xanthoma (IX), pathological intimal thickening (PIT), and fibrous cap atheroma (FCA). Quantification of the plaque components was performed by manual or semi-automatic delineation of the lumen, media, outer wall, and the respective plaque component on all histological slides using BioPix IQ software (BioPix AB, version 3.4.0).

Analysis of IVUS and OCT data was performed using QCU-CMS software (version 4.69, Leiden University Medical Center, LKEB, Division of Image Processing/MEDIS medical imaging systems BV, Leiden). ECG-gated IVUS images were analyzed approximately every 0.5 mm to assess lumen and outer wall dimensions and thus plaque size. For final analysis, data were averaged over 3 mm in longitudinal direction to reduce the influence of manual drawing errors and to reduce statistical dependence among the data points. The plaque size was also assessed by classifying the maximal intima-media thickness per 3 mm-segment into 4 grades (<0.5 mm, 0.5–0.7 mm, 0.7–1.0 mm, and >1.0 mm) according to the method of Chatzizisis et al.[9] The percentage of the segments occupied by the respective grade was quantified per artery and averaged over all arteries.

OCT data were analyzed every millimeter (1 out of 5 frames) according to consensus standards[25] as fibrous plaque, lipid-rich plaque or a FCA in pullbacks that showed at least one frame with visible plaque. Angles for individual plaque components were drawn manually.

Patient Data

EDTA plasma was collected from 3 homozygous *LDLR* mutation FH patients who were treated at the Erasmus MC, the Netherlands. All patients provided written informed consent, and the collection of blood was approved by the Medical Ethical Committee of the Erasmus MC (MEC, 2012–309).

Lipoprotein Profiling

EDTA plasma and serum collected from the pigs at T_1, T_2, and T_3 was used to perform lipoprotein profiling by density-gradient ultracentrifugation (DGUC) and size-exclusion chromatography (fast-protein liquid chromatography [FPLC]). Cholesterol and triglyceride levels were determined in all gradient or elution fractions using standard laboratory methods. Sphingolipid (ceramides [Cer], sphingosine-1-phosphate [S1P], and sphingomyelin [SM]) content of the total plasma and of the LDL fractions was measured using high-pressure liquid chromatography mass-spectrometry analyses. For analysis, the total cholesterol (FPLC and DGUC), S1P (FPLC), ceramide (FPLC), and SM (FPLC) levels in the LDL fractions were assessed by calculating the area under the curve. Sphingolipid levels were expressed relative to the total cholesterol levels in the respective lipoprotein pools. Also the Cer(d18:1/16:0)/Cer(d18:1/24:0), Cer(d18:1/18:0)/Cer(d18:1/24:0), and Cer(d18:1/24:1)/Cer(d18:1/24:0) ratios were assessed within the LDL fractions.[26]

To identify different LDL subpopulations, the lipoproteins from pig plasma samples and from the patient with homozygous FH plasma samples were first separated on density by

Downloaded from http://ahajournals.org by on November 7, 2019

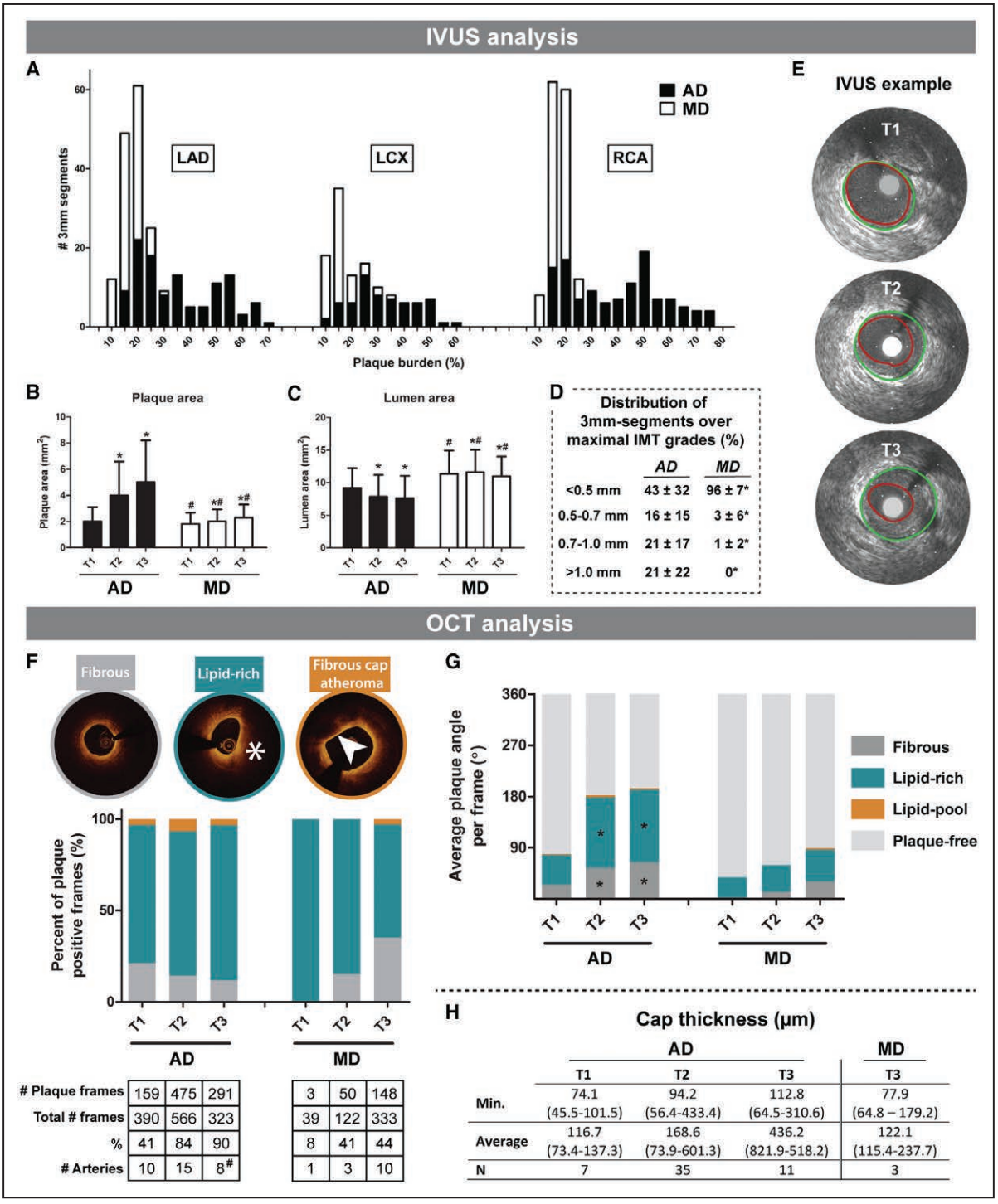

Figure 1. In vivo intravascular ultrasound (IVUS) and optical coherence tomography (OCT) analysis of coronary plaque development. IVUS analysis (**A**–**E**): **A**, Stacked histogram of the number of 3 mm segments (*y* axis) with a corresponding PB (%) at the last imaging time point (*x* axis) of the advanced-diseased pigs (ADs; black bars) and mildly diseased pigs (MDs; white bars) in the left anterior descending coronary artery (LAD), left circumflex coronary artery (LCX), and right coronary artery (RCA). **B** and **C**, Change of plaque area (PA; mm²; **B**) and lumen area (LA; **C**) between T1 and T3 (mean±SD). *P<0.05 compared with T1. #P<0.05 between MDs and ADs at the corresponding time point. **D**, Average percentage (±SD) of the number of 3 mm segments per artery that displayed one of the maximal intima-media thickness (IMT) grades at the last imaging time point. *P<0.05 compared with FRs. **E**, Example IVUS images of plaque growth between T1 and T3 at one location in an AD pig. Vessel wall (green) and lumen border (red) are indicated. OCT analysis (**F**–**H**): **F**, Average percentage of a fibrous, lipid-rich (*) or fibrous cap atheroma (FCA; arrowhead points out lipid-pool with overlying fibrous cap) of all plaque positive frames for T1 to T3. The total number of plaque positive frames and arteries is depicted under the figure. #Note that at T3, data of 2 highly atherosclerotic AD pigs are missing due to early sacrifice after T2. **G**, The average angle of fibrous plaque, lipid-rich plaque, or lipid-pool per frame at T1 to T3. **H**, Median (range) cap thickness values derived from the frames presenting with a lipid-pool (ie, FCA). The minimal (Min.) and average thickness, and the number of fibrous caps are displayed.

Downloaded from http://ahajournals.org by on November 7, 2019

DGUC. From these density-gradients, the LDL fractions were isolated and subsequently separated on size by FPLC.

Statistics

IBM SPSS Statistics (version 21.0) software was used for statistical analysis. Non-normal distributed data are presented as median (range), and statistical difference was determined with the Mann-Whitney *U* test. Normally, distributed data are shown as mean±SD, and significance was determined using an unpaired Student *t* test, a repeated-measures ANOVA with post hoc testing (Bonferroni) or a paired Student *t* test. Difference in the frequency distribution of different plaque categories was tested using a χ^2 test or a Fisher exact test. Absolute values subtracted from imaging and histological data were averaged per artery. For categorical multiple group comparison, z-scores >1.96 were regarded significant. For all other tests, $P<0.05$ was regarded to indicate statistical significance.

RESULTS

General Model Characteristics

The weight of the pigs remained constant during the follow-up period at 86 kg (60–104 kg). After 3 months of atherogenic diet, a significant increase in total cholesterol (from 1.9 mmol/L [1.8–2.2 mmol/L] to 10.4 mmol/L [8.9–22.3 mmol/L]), LDL-C (LDL-cholesterol; from 1.5 mmol/L [1.4–1.8 mmol/L] to 8.8 mmol/L [6.7–23.3 mmol/L]) and HDL-C (HDL-cholesterol) levels (from 0.3 mmol/L [0.2–0.3 mmol/L] to 2.9 mmol/L [2.1–4.9 mmol/L]) was observed compared the levels before atherogenic diet ($P<0.05$).

Advanced and Mildly Diseased Pigs: General Characteristics and In Vivo IVUS Measurements of Plaque Size and Plaque Growth

Five of the 10 pigs displayed development of large, lumen intruding plaques in the coronary arteries (maximal plaque burden 69% [57%–77%]; advanced-diseased pigs [ADs]) while the other 5 pigs showed limited plaque development (maximal plaque burden 25% [23%–34%]; mildly diseased pigs [MDs]; Figure 1A). Although the animals were run in 2 subsequent groups, the distribution of the AD/MD animals over both groups appeared random (Group 1: 2/6; Group 2: 3/5 [ADs/total number of animals]), ruling out the effect of factors like housing, diet, seasonal period or birth-year. Since the difference in plaque development between both groups was so pronounced, all subsequent results are presented separately for the MDs and the ADs.

In the ADs, plaque area was markedly larger, and lumen area was smaller compared with the MDs ($P<0.05$; Figure 1B and 1C). The ADs demonstrated significant increase in plaque area (Figure 1B) and decrease in lumen area (Figure 1C) at T_2 and T_3 compared with T_1 ($P<0.05$). In the MDs, plaque growth (Figure 1B) was limited but still significant ($P<0.05$), while the lumen area (Figure 1C) showed a slight increase from T_1 to T_2 ($P<0.05$) and a decrease at T_3 ($P<0.05$).

At the last time point, on average 21% of the analyzed segments of the ADs was occupied by plaques with a maximal intima-media thickness >1.0 mm while in the MDs none of the segments demonstrated plaques with this intima-media thickness grade (Figure 1D).

Plaque Classification by OCT

The percentage of OCT frames that presented with plaque increased over time in both the MD and AD pigs (Figure 1F). The large majority of the OCT-detected plaques presented as lipid-rich, and this distribution did not change over time (Figure 1F). OCT-observed FCAs were rare. In ADs, OCT-FCA occurrence increased between T_1 and T_2 from 4.4% (7 frames) to 7.4% (35 frames) of the total number of frames with plaque ($P=0.001$) and tended to decrease again at T_3 to 3.8% (11 frames; $P=0.07$; Figure 1F). This latter observation is explained by the loss of 2/5 AD pigs before T_3 which demonstrated the majority of OCT-FCAs (57%) at T_2. In the MDs, OCT-FCAs were only observed at T_3 in 2.0% (3 frames) of the total number of frames with plaque. In a more detailed analysis, the ADs displayed an increase in the average total plaque angle between T_1 and T_2 which could mainly be attributed to the increase in both fibrous and lipid-rich angles ($P<0.05$; Figure 1G). Furthermore, there was a small, but nonsignificant increase in the lipid-pool angle. Between T_2 and T_3, both the average plaque angle and the composition remained constant in the ADs which can again be explained by the loss of 2 AD pigs with the most advanced plaques at T_2. The MDs displayed a small, but nonsignificant increase in average plaque angle and no significant changes in plaque composition were observed (Figure 1G). Cap thickness was determined in OCT-FCAs (Figure 1H) and in the ADs, respectively 2 (T_1), 3 (T_2), and 1 (T_3) frames presented with a thin-fibrous cap (<65 μm). In the MDs, one frame with a thin-FCA was observed and only at T_3.

Histological Characterization of the Coronary Atherosclerotic Plaques

Plaque Classification and Localization

In total, 580 coronary 3 mm segments were analyzed by histology: 297 segments from ADs and 283 segments from MDs, with on average 19±6 segments per artery. In the ADs, the presence of a healthy vessel wall or a vessel wall with IT was rare, while IX, PIT, and FCA were each present in approximately one-third of all analyzed segments (Figure 2A). For the MDs, IX was the most frequently observed plaque type, covering 73.5%

Downloaded from http://ahajournals.org by on November 7, 2019

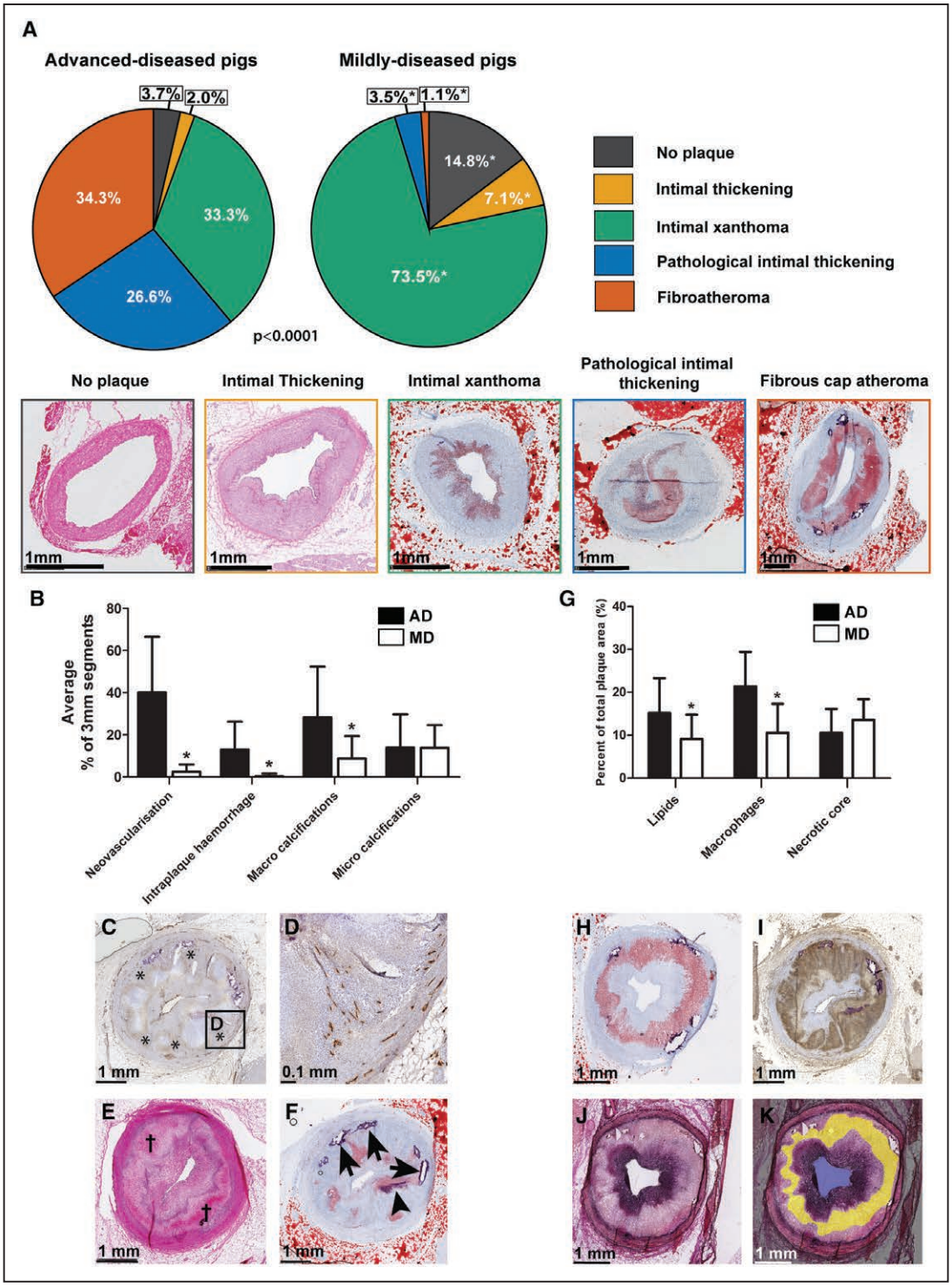

Figure 2. Histological quantification of coronary plaque classification and components.
A, Quantification of the frequency of occurrence of the different plaque types. Data are presented as a percentage of the total number of segments, separately for the mildly diseased pigs (MDs; 283 3 mm segments) and advanced-diseased pigs (AD) pigs (297 3 mm-segments). *z-score >1.96 compared with ADs. Bottom of the figure: example images of the respective plaque types: no plaque and intimal thickening: HE-staining; other plaque types: Oil-red-O staining (red=lipids and purple=calcifications). **B**, Mean (±SD) percentage of 3 mm segments per artery that contained the respective plaque component in ADs (black bars) and MDs (white bars). *$P<0.05$. **C**–**F**, Histological examples of the plaque components quantified in the bar graph. **C**, Neovascularisation (*, CD31-staining: brown), (**D**) magnification of (**C**). **E**, Intraplaque hemorrhage (†, HE-staining). **F**, Lipids (Oil-red-O staining: red), microcalcifications (arrowhead), and macrocalcifications (arrows). **G**, Mean (±SD) area percentage per artery of the respective plaque component in ADs (black bars) and MDs (white bars) in segments positive for that plaque component. *$P<0.05$ compared with ADs. **H**–**K**, Example images of: (**H**) lipids (Oil-red-O staining; red); (**I**) macrophages (CD68 staining: brown); (**J**) collagen (Miller staining: purple). The Miller staining was used to delineate the necrotic core (indicated in yellow in [**K**]).

Downloaded from http://ahajournals.org by on November 7, 2019

of the segments. The frequency of the various plaque classes differed significantly between the ADs and MDs (χ^2=211.0, P<0.0001; Figure 2A).

The plaque area of each respective plaque type did not differ between AD and MD pigs (Table 1), while the intima/media ratio for segments with PIT was significantly higher in the AD than the MD pigs.

In the ADs, the anatomic distribution of the various plaque types differed significantly over the coronary arteries with a higher frequency of FCAs in the proximal part of the arteries compared with the distal part (χ^2=39.6, P<0.0001). In contrast, the plaque type distribution in the MDs was more homogenous (Figure IA in the online-only Data Supplement). Mainly for the MDs, the presence of a side branch coincided with a trend towards a more advanced plaque type (Figure IB in the online-only Data Supplement). In comparison with the left anterior descending and right coronary artery, the left circumflex presented with more early-stage plaques which were most apparent in the MDs (Figure IC in the online-only Data Supplement).

Quantification of Plaque Components

Neovascularization, intraplaque hemorrhage, and macrocalcifications were frequently observed in the ADs and were rare in the MDs (P<0.05), while micro-calcifications were equally present (Figure 2B through 2F). Furthermore, coronary segments obtained from the ADs contained a significantly larger area percentage of lipids and macrophages compared with the MDs (Figure 2G through 2I) when the component was present. In necrotic core positive segments, the necrotic core area percentage did not differ (Figure 2G, 2J, and 2K), but necrotic cores were much more frequently present in plaques from ADs (102 segments, 34%) compared with MDs (3 segments, 1%).

Lipoprotein Profiling of the Advanced and Mildly Diseased Pigs

The ADs and MDs carried the same *LDLR* mutation were fed the same amount of atherogenic diet and displayed no differences in conventional risk factors such as weight, total cholesterol levels, leucocyte count (inflammation), LCL-C, HDL-C, and the ratio of LDL-C/HDL-C (Table I in the online-only Data Supplement). To increase understanding of the large differences in coronary plaque development between the MD and AD pigs, detailed lipoprotein profiling was performed.

Detection of Regular LDL and Larger LDL at T_1

Separation of the plasma lipoproteins by density (DGUC) showed high LDL-C levels and relatively low HDL-C and VLDL-C (very-low density lipoprotein cholesterol) levels (Figure II in the online-only Data Supplement) in all pigs. AD and MD pigs demonstrated no significant differences in total LDL-C in DGUC at T_1 (area under the curve, 7.1 [4.5–18.1] versus 7.1 [5.1–10.3]; Figure II in the online-only Data Supplement). Separation of the plasma lipoproteins by size (FPLC), however, revealed a marked difference in distribution of cholesterol over the lipoproteins between AD and MD pigs which was most pronounced in the fractions expected to contain LDL-C and VLDL-C (Figure 3A and Figure II in the online-only Data Supplement). While cholesterol was detected at both the LDL and VLDL location in the FPLC fractions, the lipoproteins at the VLDL location did not contain triglycerides (Figure II in the online-only Data Supplement). Since VLDL is characterized by high levels of triglycerides (as for example observed in human pool plasma, Figure II in the online-only Data Supplement), the almost absent triglycerides at the VLDL location suggest that the observed larger lipoprotein subpopulation is highly unlikely to be VLDL. In line with this, the DGUC profiles showed hardly any cholesterol in the fractions in the VLDL-density range (Figure II in the online-only Data Supplement). To further elucidate the origin of the larger-sized lipoproteins, we isolated the DGUC LDL fractions and subsequently separated these fractions on size by FPLC. This analysis excluded the presence of VLDL and revealed the presence of LDL within the size-range of regular LDL, but also of LDL within the size-range of VLDL (Figure 3B). Based on these data, we will from now on call the specific lipoprotein subclass with the density of LDL, but the size of VLDL: larger LDL.

In the AD pigs, the regular/larger LDL-C ratio was significantly and consistently higher than in MD pigs at T_1 (Table 2).

Sphingolipid Content of Regular and Larger LDL at T_1

Next, the sphingolipid content of the 2 LDL subclasses was determined and expressed relative to the cholesterol concentration. In the ADs, the Cer(d18:1/18:0) content of the larger LDL was significantly higher than in MDs (Table 3). Furthermore, the regular/larger LDL ratios of S1P(d18:1), Cer(d18:1/16:0), and Cer(d18:1/18:0) were significantly lower in the ADs than in the MDs. Cer(d18:1/14:0) showed a similar trend (Table 3). These results indicate relatively higher S1P and long-chain ceramide levels in larger LDL and lower levels in regular LDL of the AD pigs compared with the MD pigs. Moreover, compared with the MDs, a lower ratio of Cer(d18:1/16:0)/Cer(d18:1/24:0; P=0.10) and Cer(d18:1/18:0)/Cer(d18:1/24:0; P=0.03) was observed in regular over larger LDL in ADs (Table II in the online-only Data Supplement). This indicated that in the ADs, larger LDL contained relatively more long-chain ceramides (Cer[d18:1/16:0] and Cer[d18:1/18:0]) and less very long-chain ceramides (Cer[d18:1/24:0]) compared with regular LDL, whereas in MDs there were relatively less long-chain ceramides in relation to very-long-chain ceramides. No differences were found in the Cer(d18:1/24:1)/Cer(d18:1/24:0) ratio in regular over

Downloaded from http://ahajournals.org by on November 7, 2019

Table 1. Plaque Area and Intima-Media Ratio for Every Plaque Type as Determined by Histology

	Advanced-Diseased Pigs				Mildly Diseased Pigs			
	IT	*IX*	*PIT*	*FCA*	*IT*	*IX*	*PIT*	*FCA*
PA, mm^2	0.90±1.12	0.92±0.60	2.09±0.90	4.23±1.38	0.69±0.55	0.75±0.34	1.78±0.65	3.38±2.25†
IMR	0.63±0.68	0.69±0.35	1.78±0.48	2.56±0.70	0.35±0.23	0.54±0.36	1.06±0.38*	1.48±0.74†

FCA indicates fibrous cap atheroma; IMR, intima/media ratio; IT, intimal thickening; IX, intimal xanthoma; PA, plaque area; and PIT, pathological intimal thickening.
*P<0.05 compared with the same plaque type of the advanced-diseased pigs.
†FCA in mildly diseased pigs: n=3, no statistics performed on this category.

larger LDL (Table II in the online-only Data Supplement) between ADs and MDs.

With regard to the SMs, the SM(d18:1/16:0) and SM(d18:1/18:0) content was higher in larger LDL of ADs than of MDs (Table 4). A similar trend was observed for SM(18:1/20:0; P=0.06). Following the first 2 observations, also the regular/larger LDL ratios of SM(d18:1/16:0) and SM(d18:1/18:0) were significantly lower in the AD pigs than in the MD pigs. This same significant difference was observed for the SM total regular/larger ratio (Table 4).

Cholesterol and Sphingolipid Content of Regular and Larger LDL at T_2 and T_3

As for the T_1 plasma samples, we determined the cholesterol and sphingolipid content of the 2 LDL subtypes in the plasma samples taken at T_2 and T_3. In contrast to the findings of T_1, no differences were observed in the distribution of cholesterol over regular and larger LDL between both groups of pigs at T_2 and T_3 (Table III in the online-only Data Supplement). For the sphingolipid content, no differences were found in the distribution of both ceramides and SMs over regular and larger LDL (Tables IV through

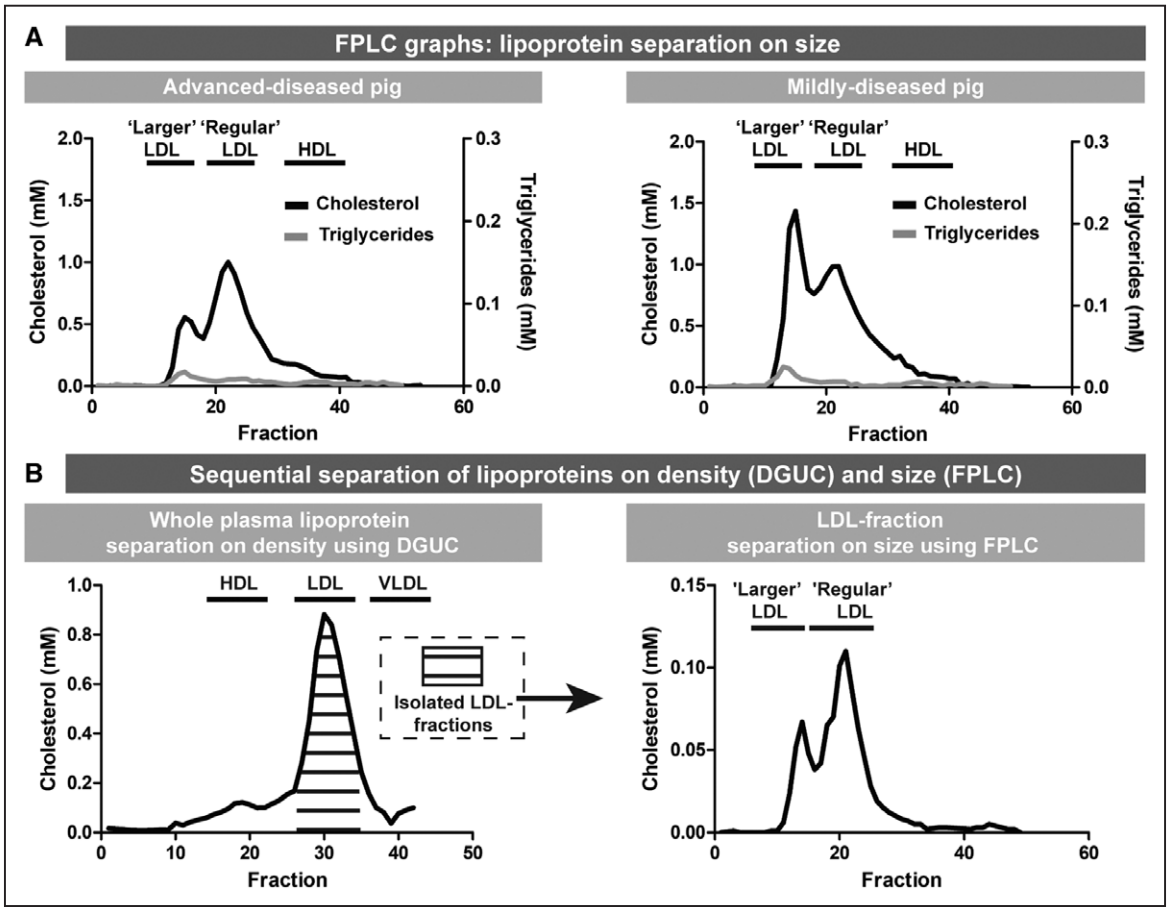

Figure 3. Distinct lipoprotein profile with larger and regular LDL (low-density lipoprotein) associated with coronary atherosclerosis disease severity at T1.
A, Representative fast-protein liquid chromatography (FPLC) profiles of one advanced-diseased pig (AD) and one mildly diseased pig. Both the cholesterol levels (black line) and the triglyceride levels (gray line) are indicated. Larger LDL has the same size as VLDL (very-low–density lipoproteins). **B**, Sequential separation of lipoproteins using density-gradient ultracentrifuge (DGUC) and FPLC (graph of one example AD pig). Lipoproteins were separated on density using DGUC. Subsequently, the pooled LDL fractions were subjected to FPLC revealing the presence of regular LDL and larger LDL. HDL indicates high-density lipoprotein.

Downloaded from http://ahajournals.org by on November 7, 2019

Table 2. Cholesterol Content of Regular and Larger LDL

	Advanced-Diseased Pigs	Mildly Diseased Pigs	*P* Value
Cholesterol regular LDL	6.3 (6.1–17.7)	7.3 (3.6–7.7)	1
Cholesterol larger LDL	1.9 (1.3–5.3)	5.0 (2.3–7.3)	0.22
Ratio cholesterol regular/larger LDL	3.3 (2.5–4.7)	1.5 (1.1–1.8)	0.008*

Data presented as median (range) of the area under the curve. LDL indicates low-density lipoprotein.
*Significant values.

IX in the online-only Data Supplement). The total plasma levels of Cer(18:1/18:0) and Cer(18:1/24:0) were, however, higher in the AD than in the MD animals at T_2 (Table IV in the online-only Data Supplement).

LDL Profile in Patients With Homozygous FH

Clinical characteristics of the 3 homozygous patients with FH, all carrying *LDLR* mutations, are described in Table X in the online-only Data Supplement. Isolation of LDL by DGUC and subsequent separation of the isolated LDL fractions by FPLC revealed the presence of regular and larger LDL in the plasma of all 3 patients with homozygous FH. The LDL profiles of patient 2 and 3 were similar to the T_1 LDL profiles of the ADs with higher regular LDL-C levels compared with larger LDL-C levels while patient 1 displayed an LDL-C profile similar to MDs (Figure 4).

DISCUSSION

Our main findings were that: (1) on an atherogenic diet, plaques in all homozygous FH pigs progressed significantly, but we could distinguish MDs and ADs, despite the presence of the same homozygous *LDLR* R84C mutation and similar cholesterol, LDL-C, HDL-C, and inflammatory levels; (2) the plaques of the MDs progressed to a stage of IX while in the ADs, large, advanced plaques with vulnerable characteristics including lipid-rich necrotic cores, calcifications, neovascularization, and intraplaque hemorrhage were frequently observed; (3) separation of plasma lipoproteins based on size revealed a distinct LDL profile which differed significantly between ADs and MDs at T_1. This LDL profile contained both regular LDL and lipoproteins with the density of LDL and the size of VLDL, that is, larger LDL; (4) the distribution of cholesterol and sphingolipids over regular and larger LDL shortly after the start of the atherogenic diet could significantly and consistently be linked to the severity of subsequent coronary atherosclerosis development; (5) the distinct LDL profile with larger and regular LDL was also observed in plasma of homozygous patients with FH.

Coronary Atherosclerosis Development: Comparison With Other Pig Models

Although the MD pigs in our study did develop early plaques with a growth rate consistent to humans (on average 0.05 mm^2/month versus 0.02 mm^2/month[27]), pigs that develop more advanced, unstable plaques are most useful for cardiovascular studies. Therefore, we compared the results from the AD pigs with data from previously published studies on pig models of nonsurgically induced coronary atherosclerosis development (Table XI in the online-only Data Supplement).

Coronary Plaque Size

In comparison with all other porcine models of diet- or genetically induced hypercholesterolemia with or without diabetes mellitus, our AD pigs present with one of the largest histological plaque sizes (Table XI in the online-only Data Supplement). Only the atherogenic diet-diabetes mellitus pig model described by Patel et al[12] presented with on average larger plaque areas (5.0 versus 8.2 mm^2). Differences in tissue processing and the lack of perfusion fixation in many studies, including ours, however, hampers a direct comparison, especially with the results of 3 studies which do use this tissue processing technique.[15,16,28]

Although the lack of perfusion fixation of the histological samples could lead to overestimation of the plaque size, invasive imaging confirmed the presence of large plaques in our animals where 21% of the artery was occupied by plaques with a maximum intima-media thickness >1.0 mm. Furthermore, IVUS-derived plaque burden is a measure that is often applied in the clinic to quantify disease burden, but is unfortunately rarely reported by other porcine model studies. Badin et al[29] and Tharp et al[30] observed average plaque burdens of 38% and 50%, respectively. We demonstrated a maximal plaque burden of 77% in the ADs, indicating the presence of lumen intruding, clinically relevant plaques.[31]

Coronary Plaque Composition

Monitoring changes in plaque composition in animal models by serial invasive imaging is vital to assess the development stage, plaque stability, and similarity to human plaques. Our OCT imaging data showed a clear increase of coronary atherosclerosis over time. The large majority of the plaques presented as lipid-rich already from the first time point, whereas lipid-pools, that is, FCAs, were rare, even at the last imaging time point. This observation is in large contrast to our histological data and might be the result of the main drawback of OCT: the inability to image beyond lipid-rich tissue.[25] According to our histological analysis, one-third of the plaques in the ADs presented as FCAs with lipid-rich necrotic cores. The majority of these FCAs were thick-cap FCAs and lipid-rich tissue, present between the lumen and the lipid-pool, could shield the lipid-pool from detection by OCT, leading to an underestimation of FCA presence by OCT.

The histologically detected advanced plaque types PIT and FCAs were observed more frequently in the ADs from our study compared with many other models described in literature,[9,10,13,14,17,28,32,33] except for the

Downloaded from http://ahajournals.org by on November 7, 2019

Table 3. S1P and Ceramide Content of Regular and Larger LDL

	Advanced-Diseased Pigs	Mildly Diseased Pigs	*P* Value
S1P(d18:1) total plasma (×10⁻⁵)	12.4 (3.7–16.7)*	14.4 (7.7–17.4)	0.84
S1P(d18:1) regular LDL (×10⁻⁵)	2.7 (1.7–13.0)*	4.7 (1.3–6.4)	0.42
S1P(d18:1) larger LDL (×10⁻⁵)	4.7 (2.9–17.2)*	3.6 (1.4–7.9)	0.56
S1P(d18:1) regular/larger LDL	0.6 (0.5–0.8)*	0.9 (0.8–1.3)	0.016†
Cer(d18:1/14:0) total plasma (×10⁻⁵)	0.9 (0.4–1.2)	0.7 (0.4–1.1)	1
Cer(d18:1/14:0) regular LDL (×10⁻⁵)	0.6 (0.4–1.0)	0.6 (0.3–1.1)	1
Cer(d18:1/14:0) larger LDL (×10⁻⁵)	1.1 (0.9–1.6)	0.6 (0.4–1.5)	0.42
Cer(d18:1/14:0) regular/larger LDL ratio	0.6 (0.4–0.8)	0.8 (0.7–0.9)	0.06
Cer(d18:1/16:0) total plasma (×10⁻⁵)	7.3 (3.4–11.1)	6.9 (3.7–9.3)	0.69
Cer(d18:1/16:0) regular LDL (×10⁻⁵)	13.3 (4.7–14.7))	9.2 (5.2–12.6)	0.55
Cer(d18:1/16:0) larger LDL (×10⁻⁵)	19.7 (7.9–21.6)	11.9 (6.3–13.0)	0.31
Cer(d18:1/16:0) regular/larger LDL ratio	0.7 (0.6–0.7)	0.8 (0.8–1.1)	0.008†
Cer(d18:1/18:0) total plasma (×10⁻⁵)	2.4 (1.2–3.8)	1.7 (1.4–2.6)	0.55
Cer(d18:1/18:0) regular LDL (x10⁻⁵)	5.3 (2.2–7.8)	3.0 (2.6–6.7)	0.69
Cer(d18:1/18:0) larger LDL (×10⁻⁵)	7.9 (4.0–11.8)	3.8 (2.8–4.4)	0.032†
Cer(d18:1/18:0) regular/larger LDL ratio	0.6 (0.5–0.7)	1.0 (0.7–1.5)	0.008†
Cer(d18:1/20:0) total plasma (×10⁻⁵)	8.9 (3.6–14.8)	7.2 (6.5–14.7)	0.84
Cer(d18:1/20:0) regular LDL (×10⁻⁵)	5.0 (2.0–5.9)	3.5 (2.7–6.6)	0.55
Cer(d18:1/20:0) larger LDL (×10⁻⁵)	6.1 (2.8–8.9)	5.3 (3.7–7.0)	0.55
Cer(d18:1/20:0) regular/larger LDL ratio	0.8 (0.7–0.9)	0.7 (0.6–0.9)	0.69
Cer(d18:1/22:0) total plasma (×10⁻⁵)	20.9 (9.7–38.7)	18.3 (13.8–36.4)	1
Cer(d18:1/22:0) regular LDL (×10⁻⁵)	8.2 (3.8–11.9)	6.0 (4.8–12.1)	0.55
Cer(d18:1/22:0) larger LDL (×10⁻⁵)	13.5 (5.9–17.2)	9.6 (6.5–13.9)	0.55
Cer(d18:1/22:0) regular/larger LDL ratio	0.7 (0.6–0.9)	0.7 (0.6–0.9)	1
Cer(d18:1/24:0) total plasma (×10⁻⁵)	20.8 (11.8–35.3)	17.1 (12.8–32.8)	1
Cer(d18:1/24:0) regular LDL (×10⁻⁵)	11.1 (7.7–11.9)	8.3 (6.1–13.2)	0.31
Cer(d18:1/24:0) larger LDL (×10⁻⁵)	16.3 (12.4–18.8)	13.5 (9.8–15.9)	0.15
Cer(d18:1/24:0) regular/larger LDL ratio	0.62 (0.5–0.8)	0.62 (0.6–0.9)	0.69
Cer(d18:1/24:1) total plasma (×10⁻⁵)	19.9 (11.3–24.9)	16.5 (12.8–32.3)	1
Cer(d18:1/24:1) regular LDL (×10⁻⁵)	10.8 (6.3–12.7)	7.6 (6.7–13.4)	0.69
Cer(d18:1/24:1) larger LDL (×10⁻⁵)	14.9 (8.4–16.3)	12.6 (8.5–14.7)	0.22
Cer(d18:1/24:1) regular/larger LDL ratio	0.7 (0.7–0.8)	0.7 (0.6–1.0)	1
Cer Total total plasma (×10⁻⁵)	80.4 (41.5–120.7)	66.8 (52.7–128.8)	0.84
Cer Total regular LDL (×10⁻⁵)	54.2 (27.6–58.8)	38.7 (29.9–62.7)	0.55
Cer Total larger LDL (×10⁻⁵)	77.6 (43.3–85.3)	58.1 (38.6–65.0)	0.10
Cer Total regular/larger LDL ratio	0.7 (0.6–0.8)	0.8 (0.7–1.0)	0.22

All sphingolipid data were expressed relative to the cholesterol concentration in total plasma or the respective LDL peak. Data are presented as median (range) of the area under the curve. LDL indicates low-density lipoprotein.

*Significant values.

†Data of 1 pig are missing.

atherogenic diet-diabetes mellitus model by Patel et al[12] (Table XI in the online-only Data Supplement), confirming that the advanced disease stage observed in our model is very rare.

Besides a generally advanced plaque type, ADs displayed important features of unstable plaques.[24] Several of the previously studied porcine models also present with plaques that display necrotic cores, calcifications, and neovascularisation,[8–10,14,17,34] although quantification is often not reported. While some articles also report the occurrence of intraplaque hemorrhage,[8,15,17,34] the AD pigs in this study present widespread intraplaque hemorrhage, known to be an important indicator of fast plaque growth and destabilization.[35]

While the MD pigs displayed more diffuse disease development, AD pigs developed the largest and most advanced plaques mainly in the proximal coronary regions. This latter observation very well matches the coronary atherosclerosis growth patterns observed in humans.[36]

Taken together, the AD pigs of the adult FBM minipig model from this study develop some of the most advanced plaques so far described in literature, and this model is not complicated by the introduction of extra risk factors like diabetes mellitus.[12] The development of the large plaques with unstable, human-like features as observed in the AD pigs is likely associated with the advanced age of the animals. Unlike almost all previous studies (Table XI in the online-only Data Supplement), we used adult pigs instead of juveniles for our experiments. As mentioned in the introduction, the adult age greatly improves the resemblance to human disease pathophysiology, and aging is known to enhance atherosclerosis development both in pigs[29] and

Downloaded from http://ahajournals.org by on November 7, 2019

Table 4. Sphingomyelin Content of regular and larger LDL

	Advanced-Diseased Pigs	Mildly Diseased Pigs	*P* Value
SM(d18:1/16:0) total plasma (×10⁻³)	17.0 (8.0–17.4)	13.4 (11.4–22.6)	0.55
SM(d18:1/16:0) regular LDL (×10⁻³)	26.1 (21.4–28.6)	24.0 (20.2–26.4)	0.42
SM(d18:1/16:0) larger LDL (×10⁻³)	36.9 (34.9–41.6)	25.8 (22.3–35.1)	0.032*
SM(d18:1/16:0) regular/larger LDL	0.7 (0.6–0.7)	0.8 (0.8–1.1)	0.008*
SM(d18:1/18:0) total plasma (×10⁻³)	2.9 (1.2–3.0)	2.6 (1.7–3.9)	0.55
SM(d18:1/18:0) regular LDL (×10⁻³)	4.1 (2.8–5.4)	3.3 (2.9–4.0)	0.31
SM(d18:1/18:0) larger LDL (×10⁻³)	5.5 (4.5–7.0)	4.3 (3.0–5.1)	0.032*
SM(d18:1/18:0) regular/larger LDL ratio	0.7 (0.6–0.8)	0.8 (0.7–1.1)	0.008*
SM(d18:1/18:1) total plasma (×10⁻³)	0.6 (0.3–0.7)	0.4 (0.3–0.9)	0.55
SM(d18:1/18:1) regular LDL (×10⁻³)	0.7 (0.5–0.9)	0.6 (0.4–0.8)	0.22
SM(d18:1/18:1) larger LDL (×10⁻³)	1.0 (0.9–1.2)	0.7 (0.5–1.0)	0.10
SM(d18:1/18:1) regular/larger LDL ratio	0.8 (0.5–0.8)	0.8 (0.7–1.1)	0.31
SM(d18:1/20:0) total plasma (×10⁻³)	3.9 (1.5–4.2)	4.3 (2.6–5.7)	0.31
SM(d18:1/20:0) regular LDL (×10⁻³)	3.5 (2.5–4.0)	3.3 (2.5–4.5)	0.84
SM(d18:1/20:0) larger LDL (×10⁻³)	5.0 (4.4–5.7)	4.5 (3.0–5.5)	0.31
SM(d18:1/20:0) regular/larger LDL ratio	0.7 (0.6–0.8)	0.8 (0.7–1.1)	0.06
SM(d18:1/22:0) total plasma (×10⁻³)	6.3 (4.4–7.5)	6.4 (5.0–9.0)	0.55
SM(d18:1/22:0) regular LDL (×10⁻³)	4.3 (4.0–5.2)	4.6 (3.7–4.8)	1.0
SM(d18:1/22:0) larger LDL (×10⁻³)	5.3 (4.8–7.6)	5.6 (4.2–6.4)	0.55
SM(d18:1/22:0) regular/larger LDL ratio	0.8 (0.7–0.8)	0.8 (0.8–1.1)	0.31
SM(d18:1/24:0) total plasma (×10⁻³)	3.3 (2.7–4.7)	3.7 (2.8–4.9)	0.31
SM(d18:1/24:0) regular LDL (×10⁻³)	2.1 (1.4–2.4)	1.6 (1.1–2.0)	0.22
SM(d18:1/24:0) larger LDL (×10⁻³)	2.5 (1.8–2.8)	2.0 (1.5–2.7)	0.31
SM(d18:1/24:0) regular/larger LDL ratio	0.8 (0.8–0.9)	0.8 (0.6–1.0)	0.84
SM(d18:1/24:1) total plasma (×10⁻³)	14.6 (13.6–20.1)	16.5 (12.3–21.4)	0.69
SM(d18:1/24:1) regular LDL (×10⁻³)	10.7 (8.5–14.8)	10.2 (7.1–11.0)	0.31
SM(d18:1/24:1) larger LDL (×10⁻³)	12.9 (11.4–17.0)	12.1 (9.4–14.4)	0.55
SM(d18:1/24:1) regular/larger LDL ratio	0.7 (0.7–0.9)	0.8 (0.7–1.0)	1.0
SM Total total plasma (×10⁻³)	46.5 (36.5–56.4)	47.2 (36.1–68.3)	0.84
SM Total regular LDL (×10⁻³)	50.7 (47.1–61.1)	47.8 (38.1–52.4)	0.69
SM Total larger LDL (×10⁻³)	72.4 (65.2–80.7)	54.9 (44.4–69.7)	0.10
SM Total regular/larger LDL ratio	0.7 (0.7–0.8)	0.8 (0.8–1.1)	0.03*

All sphingolipid data were expressed relative to the cholesterol concentration in total plasma or the respective LDL peak. Data are presented as median (range) of the area under the curve. LDL indicates low-density lipoprotein.

*Significant values.

in humans.[19–21] The extensive characterization of coronary atherosclerosis development in this model forms a road-map for future pathophysiological or imaging studies with this highly relevant model. Selection of the ADs on forehand by using the described lipoprotein profiling would further accommodate this. Future studies will have to provide more information on sex-dependent differences and a possible genetic basis and heredity of the observed inter-individual differences in disease development.

The Distribution of Cholesterol and Sphingolipids Over LDL Subclasses Is Directly Linked to the Severity of Subsequent Coronary Atherosclerosis Development

Although inter-individual variation in CAD development has been previously observed in patients with FH[22] as well as in other animal models of FH, such a pronounced difference in disease development as observed in our pig model has, to the best of our knowledge, not been reported before. Conventional risk factors such as total cholesterol, LDL-C, and inflammatory markers could not distinguish AD from MD pigs. Detailed lipoprotein analysis, performed to elucidate possible underlying mechanisms, however, revealed an LDL profile with regular and larger LDL in FH pigs shortly after the start of the atherogenic diet that was distinctly different between MD and AD pigs.

LDL is an established and important initiator and promotor of atherosclerosis and remains the primary target of prevention of CAD.[37] Not only the concentration of circulating LDL determines the risk of CAD, also differences in size, density, and composition can influence its atherogenicity.[38] For example, predominance of small-dense LDL has been strongly correlated with an increased risk of CAD.[39] Besides smaller LDL, in previous studies, also the shift towards larger, triglyceride-rich IDL (intermediate-density lipoproteins)-sized lipoproteins has been linked to the occurrence of myocardial infarction.[40] In our current study, the observed LDL-C profile with regular and larger LDL distinguished AD from MD pigs in all cases.

Downloaded from http://ahajournals.org by on November 7, 2019

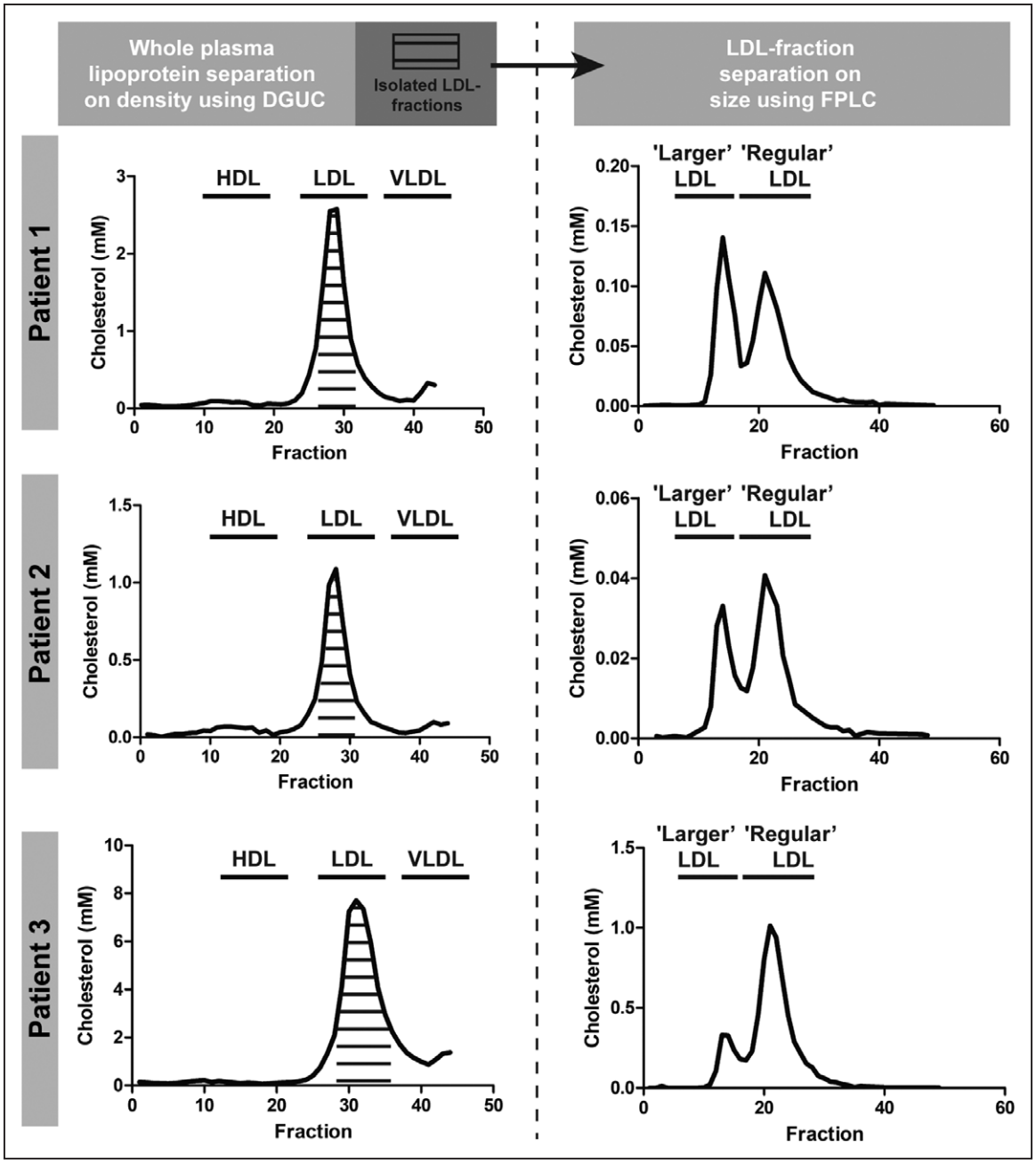

Figure 4. Low-density lipoprotein (LDL) profiles of 3 patients with homozygous familial hypercholesterolemia (FH). Lipoproteins were separated on density using density-gradient ultracentrifuge (DGUC). Subsequently, the pooled LDL fractions were subjected to fast-protein liquid chromatography (FPLC) revealing the presence of regular LDL and larger LDL in patients with homozygous FH. HDL indicates high-density lipoprotein; and VLDL, very-low–density lipoproteins.

Different from other studies that describe the occurrence of triglyceride-rich larger LDL (ie, IDL), the larger LDL particles we observed were similar in size to VLDL. We still considered these particles to be LDL because of the very low triglyceride levels after size separation and the very low levels of VLDL-C after density gradient ultracentrifugation. Lipoproteins with the density of LDL, with the size of VLDL and with low triglyceride levels have been observed before in atherosclerotic tissue homogenates[41] and in plasma of atherogenic diet-fed pigs with an *LDLR*-mutation[15] (same breed used in this study) and with an *PCSK9*-mutation.[17] However, this larger LDL has not been linked to disease severity before.

Besides cholesterol, also the distribution of sphingolipids over larger and regular LDL was significantly different between AD and MD pigs at T_1 which could indicate a difference in LDL functionality. For S1P, the regular/larger LDL ratio was higher in ADs than in MDs. Furthermore, both the long-chain ceramide and long-chain SM content were relatively higher in larger LDL of the ADs compared

Downloaded from http://ahajournals.org by on November 7, 2019

with the MDs. Sphingolipids, like SMs, S1P and ceramides, are a large group of structurally and functionally diverse lipids that are found in lipoproteins where they preserve structure and play a role in functionality of the lipoproteins. In vitro studies have shown that SM contained in LDL can undergo hydrolysis by sphingomyelinases, leading to increased LDL-ceramide levels, which in turn promotes LDL aggregation[42–44] and fusion.[44] Aggregated/fused LDL can infiltrate into the vessel wall via enhanced binding to proteoglycans.[43,44] Accordingly, LDL in atherosclerotic plaques contains markedly higher levels of ceramide compared with LDL in plasma or in the healthy vessel wall.[43,45] High levels of LDL-derived ceramides and SMs in the vessel wall can induce apoptosis,[46] foam cell formation[42,43] or increase plaque inflammation.[47] Higher LDL-ceramide and SM levels at T_1 may thus contribute to the enhanced atherosclerosis development in AD pigs.

The larger LDL observed in our FH pigs may consist of aggregated LDL as Oörni et al[44] showed that the aggregation/fusion of ceramide-rich LDL can give rise to 2 LDL subclasses upon separation by size-exclusion. This hypothesis is in line with the high SM levels observed in regular LDL of the ADs, which could make this LDL subtype more prone to aggregation. However, MD pigs presented with the highest larger LDL-C levels which contained relatively low ceramide levels, rendering aggregation unlikely.

The larger LDL of the AD and MD pigs differs in long-chain, but not in very long-chain ceramides, suggesting that besides ceramide concentration, also ceramide chain-length influences the atherogenicity. This hypothesis is strengthened by an observation by Hartmann et al[48] who reported that an increase in long-chain over very-long-chain ceramides can enhance cell proliferation and apoptosis.

The fact that we only observed the clear differences in cholesterol and sphingolipid distribution over the 2 LDL subtypes early after the start of the atherogenic diet could indicate a possible metabolic or genetic adjustment to the diet as, for example, observed by Kleeman et al.[49] However, the large differences in LDL profile present early in the study not only indicate the possible use of this profile as an early biomarker, but might also point to a causal relationship with the sensitivity for initiation of coronary atherosclerosis development.

Since the 2 different LDL subtypes can only be identified using FPLC instead of by the more commonly applied DGUC technique, a recommendation for future studies would be to characterize the components of the lipoprotein fractions also after lipoprotein separation by FPLC.

Clinical Relevance

Multiple clinical studies associated plasma-levels of ceramides and SMs with CAD development,[50] vulnerable plaque composition,[51] and with future major adverse cardiovascular events.[26,51,52] Furthermore, higher ratios of Cer(d18:1/16:0)/Cer(d18:1/24:0) and Cer(d18:1/18:0)/Cer(d18:1/24:0) have been pinpointed as predictors for cardiovascular death.[26,51] Based on the plasma levels of ceramides and SMs, we could not distinguish AD from MD pigs, possibly by a lack of power. When we, however, assessed the ceramide ratios in the 2 LDL subclasses at T_1, these were directly related to disease severity. These data suggest that assessment of the cholesterol and sphingolipid distribution over the 2 LDL subclasses is a highly potent and possibly even stronger early biomarker for individual risk assessment of coronary atherosclerosis development than LDL-C and sphingolipid levels in plasma. Future studies are necessary to further elucidate the exact composition and biological function of larger LDL, and of the importance of the regular-/larger LDL balance in atherosclerosis initiation and progression.

An interesting observation is the occurrence of the distinct LDL profile with regular and larger LDL in the plasma of 3 patients with homozygous FH in whom the LDL-C ratios displayed pronounced differences between the patients. Cardiovascular disease severity is highly variable in patients with FH and currently, no existing biomarker can reliably predict cardiovascular disease development in individual patients with FH.[53] The distinct LDL profile described in this study forms a promising early biomarker for individual patients with FH and even a potential drug target. A clinical study with a larger cohort of patients with homozygous and heterozygous FH, specifically also including women, will have to show the value of this LDL profile as a biomarker and as a risk factor for cardiovascular disease. It also needs to be determined whether this distinct LDL profile is also present in other patients with dyslipidemia and whether lipid-lowering medication like statins influences this LDL profile.

Limitations

The sample size in this study was relatively small. The division of the group of pigs with regard to disease severity was unforeseen and resulted in a low number of animals with advanced disease, but it also enabled the discovery of a new, high-potential biomarker for atherosclerosis development. Despite the low number of animals in both groups, this potential biomarker still came out as a strong, significant predictor. Furthermore, while histology was important for determining the plaque composition at a detailed level, the lack of perfusion fixation of the coronary histological samples hampered accurate quantification of plaque size. Besides, the low number of patients did not allow for a study to the relation with clinical outcome, but this first exploratory study did establish the first proof of the presence of a potential new biomarker for CAD.

Conclusions

The adult, homozygous FH FBM pig model is a large animal model in which half of the pigs allows for assessment

Downloaded from http://ahajournals.org by on November 7, 2019

of early plaque development while the other half demonstrates development of advanced coronary atherosclerotic plaques when fed an atherogenic diet. This latter group of ADs presented with widespread development of large, lumen intruding plaques with extensive unstable, human-like features. These features render these pigs very suitable for testing and validating new interventions and (invasive) imaging techniques. Besides, we identified a distinct LDL profile in which a detailed component analysis revealed that the distribution of cholesterol and sphingolipids over larger and regular LDL early after the start of the diet was directly associated with the severity of coronary atherosclerosis development. Despite the low number of pigs, these measurements were highly significantly different between both groups of pigs, indicating the power and potential of this biomarker. Since this LDL profile was already present before the start of major plaque development, there may be a causal relation with plaque initiation. This novel biomarker is highly useful to select ADs early in the study. Moreover, since we also detected this specific LDL profile in human homozygous patients with FH, this specific LDL profile might have potential to function as an early biomarker to indicate cardiovascular risk in individual (FH) patients, or to become a treatment target.

ARTICLE INFORMATION

Received April 18, 2019; accepted August 26, 2019.

Affiliations

From the Department of Cardiology, Biomedical Engineering, Erasmus MC, Rotterdam, the Netherlands (A.H., E.M.J.H., K.v.G., K.V.d.H., A.F.W.v.d.S., J.J.W.); Department of Internal Medicine, Laboratory of Vascular Medicine, Division of Pharmacology, Vascular & Metabolic Disease (S.d.H., L.v.d.Z., K.D., J.R.v.L., M.T.M.), Department of Cardiology, Experimental Cardiology (I.K.-P., M.t.L.H., D.J.D.), Department of Cardiology, Interventional Cardiology (K.T.W., J.M.R.L.), Erasmus MC, Rotterdam, the Netherlands; and Department of Angiohematology, Hospital Lariboisiere, Paris, France (L.D.).

Acknowledgments

We gratefully acknowledge Dennis Akkermans and Vincent Vaes for their help with animal caretaking and for their support during the experimental procedures. We would also like to thank Claire Bal Dit Sollier for her support in arranging the animal logistics, Frank Leijten for the genotyping of the pigs and Adrie Verhoeven for critically reviewing the article.

Sources of Funding

This work was supported by the European Research Council, Brussels, Belgium (grant agreement 310457) and by the Erasmus MC, Rotterdam, the Netherlands, Mrace pilot grant 2018.

Disclosures

K. Van der Heiden is funded by the Netherlands Heart Foundation (grant agreement NHS2014T096); S. den Hoedt is funded by ZonMW (grant agreement 733050105). The other authors report no conflicts.

REFERENCES

1. Farb A, Tang AL, Burke AP, Sessums L, Liang Y, Virmani R. Sudden coronary death. Frequency of active coronary lesions, inactive coronary lesions, and myocardial infarction. *Circulation*. 1995;92:1701–1709. doi: 10.1161/01.cir.92.7.1701
2. Kolodgie FD, Burke AP, Farb A, Gold HK, Yuan J, Narula J, Finn AV, Virmani R. The thin-cap fibroatheroma: a type of vulnerable plaque: the major precursor lesion to acute coronary syndromes. *Curr Opin Cardiol*. 2001;16:285–292.
3. Schaar JA, Muller JE, Falk E, Virmani R, Fuster V, Serruys PW, Colombo A, Stefanadis C, Ward Casscells S, Moreno PR, et al. Terminology for high-risk and vulnerable coronary artery plaques. Report of a meeting on the vulnerable plaque, June 17 and 18, 2003, Santorini, Greece. *Eur Heart J*. 2004;25:1077–1082. doi: 10.1016/j.ehj.2004.01.002
4. Getz GS, Reardon CA. Animal models of atherosclerosis. *Arterioscler Thromb Vasc Biol*. 2012;32:1104–1115. doi: 10.1161/ATVBAHA.111.237693
5. Hamamdzic D, Wilensky RL. Porcine models of accelerated coronary atherosclerosis: role of diabetes mellitus and hypercholesterolemia. *J Diabetes Res*. 2013;2013:761415. doi: 10.1155/2013/761415
6. Bourantas CV, Jaffer FA, Gijsen FJ, van Soest G, Madden SP, Courtney BK, Fard AM, Tenekecioglu E, Zeng Y, van der Steen AFW, et al. Hybrid intravascular imaging: recent advances, technical considerations, and current applications in the study of plaque pathophysiology. *Eur Heart J*. 2017;38:400–412. doi: 10.1093/eurheartj/ehw097
7. Neeb ZP, Edwards JM, Alloosh M, Long X, Mokelke EA, Sturek M. Metabolic syndrome and coronary artery disease in Ossabaw compared with Yucatan swine. *Comp Med*. 2010;60:300–315.
8. Gerrity RG, Natarajan R, Nadler JL, Kimsey T. Diabetes-induced accelerated atherosclerosis in swine. *Diabetes*. 2001;50:1654–1665. doi: 10.2337/diabetes.50.7.1654
9. Chatzizisis YS, Jonas M, Coskun AU, Beigel R, Stone BV, Maynard C, Gerrity RG, Daley W, Rogers C, Edelman ER, et al. Prediction of the localization of high-risk coronary atherosclerotic plaques on the basis of low endothelial shear stress: an intravascular ultrasound and histopathology natural history study. *Circulation*. 2008;117:993–1002. doi: 10.1161/CIRCULATIONAHA.107.695254
10. Koskinas KC, Feldman CL, Chatzizisis YS, Coskun AU, Jonas M, Maynard C, Baker AB, Papafaklis MI, Edelman ER, Stone PH. Natural history of experimental coronary atherosclerosis and vascular remodeling in relation to endothelial shear stress: a serial, *in vivo* intravascular ultrasound study. *Circulation*. 2010;121:2092–2101. doi: 10.1161/CIRCULATIONAHA.109.901678
11. Koskinas KC, Sukhova GK, Baker AB, Papafaklis MI, Chatzizisis YS, Coskun AU, Quillard T, Jonas M, Maynard C, Antoniadis AP, et al. Thin-capped atheromata with reduced collagen content in pigs develop in coronary arterial regions exposed to persistently low endothelial shear stress. *Arterioscler Thromb Vasc Biol*. 2013;33:1494–1504. doi: 10.1161/ATVBAHA.112.300827
12. Patel D, Hamamdzic D, Llano R, Patel D, Cheng L, Fenning RS, Bannan K, Wilensky RL. Subsequent development of fibroatheromas with inflamed fibrous caps can be predicted by intracoronary near infrared spectroscopy. *Arterioscler Thromb Vasc Biol*. 2013;33:347–353. doi: 10.1161/ATVBAHA.112.300710
13. Ludvigsen TP, Kirk RK, Christoffersen BØ, Pedersen HD, Martinussen T, Kildegaard J, Heegaard PM, Lykkesfeldt J, Olsen LH. Göttingen minipig model of diet-induced atherosclerosis: influence of mild streptozotocin-induced diabetes on lesion severity and markers of inflammation evaluated in obese, obese and diabetic, and lean control animals. *J Transl Med*. 2015;13:312. doi: 10.1186/s12967-015-0670-2
14. van Ditzhuijzen NS, van den Heuvel M, Sorop O, Rossi A, Veldhof T, Bruining N, Roest S, Ligthart JMR, Witberg KT, Dijkshoorn ML, et al. Serial coronary imaging of early atherosclerosis development in fast-food-fed diabetic and nondiabetic swine. *JACC Basic to Transl Sci*. 2016;1:449–460.
15. Thim T, Hagensen MK, Drouet L, Bal Dit Sollier C, Bonneau M, Granada JF, Nielsen LB, Paaske WP, Bøtker HE, Falk E. Familial hypercholesterolaemic downsized pig with human-like coronary atherosclerosis: a model for preclinical studies. *EuroIntervention*. 2010;6:261–268. doi: 10.4244/
16. Davis BT, Wang XJ, Rohret JA, Struzynski JT, Merricks EP, Bellinger DA, Rohret FA, Nichols TC, Rogers CS. Targeted disruption of LDLR causes hypercholesterolemia and atherosclerosis in Yucatan miniature pigs. *PLoS One*. 2014;9:e93457. doi: 10.1371/journal.pone.0093457
17. Al-Mashhadi RH, Sørensen CB, Kragh PM, Christoffersen C, Mortensen MB, Tolbod LP, Thim T, Du Y, Li J, Liu Y, et al. Familial hypercholesterolemia and atherosclerosis in cloned minipigs created by DNA transposition of a human PCSK9 gain-of-function mutant. *Sci Transl Med*. 2013;5:166ra1. doi: 10.1126/scitranslmed.3004853
18. Sharifi M, Futema M, Nair D, Humphries SE. Genetic architecture of familial hypercholesterolaemia. *Curr Cardiol Rep*. 2017;19:44. doi: 10.1007/s11886-017-0848-8
19. Jani B, Rajkumar C. Ageing and vascular ageing. *Postgrad Med J*. 2006;82:357–362. doi: 10.1136/pgmj.2005.036053
20. Franklin SS, Gustin W IV, Wong ND, Larson MG, Weber MA, Kannel WB, Levy D. Hemodynamic patterns of age-related changes in blood

Downloaded from http://ahajournals.org by on November 7, 2019

pressure. The Framingham Heart Study. *Circulation*. 1997;96:308–315. doi: 10.1161/01.cir.96.1.308
21. Okęcka-Szymańska J, Hübner-Woźniak E, Piątkowska I, Malara M. Effects of age, gender and physical activity on plasma lipid profile. *Biomed Hum Kinet*. 2011;3:1–5.
22. Stone NJ, Levy RI, Fredrickson DS, Verter J. Coronary artery disease in 116 kindred with familial type II hyperlipoproteinemia. *Circulation*. 1974;49:476–488. doi: 10.1161/01.cir.49.3.476
23. National Research Council (US) Committee for the Update of the Guide for Care and Use of Laboratory Animals. *Guide for the Care and Use of Laboratory Animals*, 8th edition. Guid. Care Use Lab. Anim. Washington: National Academies Press (US); 2011.
24. Virmani R, Kolodgie FD, Burke AP, Farb A, Schwartz SM. Lessons from sudden coronary death: a comprehensive morphological classification scheme for atherosclerotic lesions. *Arterioscler Thromb Vasc Biol*. 2000;20:1262–1275. doi: 10.1161/01.atv.20.5.1262
25. Tearney GJ, Regar E, Akasaka T, Adriaenssens T, Barlis P, Bezerra HG, Bouma B, Bruining N, Cho JM, Chowdhary S, et al; International Working Group for Intravascular Optical Coherence Tomography (IWG-IVOCT). Consensus standards for acquisition, measurement, and reporting of intravascular optical coherence tomography studies: a report from the International Working Group for intravascular optical coherence tomography standardization and validation. *J Am Coll Cardiol*. 2012;59:1058–1072. doi: 10.1016/j.jacc.2011.09.079
26. Laaksonen R, Ekroos K, Sysi-Aho M, Hilvo M, Vihervaara T, Kauhanen D, Suoniemi M, Hurme R, März W, Scharnagl H, et al. Plasma ceramides predict cardiovascular death in patients with stable coronary artery disease and acute coronary syndromes beyond LDL-cholesterol. *Eur Heart J*. 2016;37:1967–1976. doi: 10.1093/eurheartj/ehw148
27. Samady H, Eshtehardi P, McDaniel MC, Suo J, Dhawan SS, Maynard C, Timmins LH, Quyyumi AA, Giddens DP. Coronary artery wall shear stress is associated with progression and transformation of atherosclerotic plaque and arterial remodeling in patients with coronary artery disease. *Circulation*. 2011;124:779–788. doi: 10.1161/CIRCULATIONAHA.111.021824
28. Poulsen CB, Al-Mashhadi AL, von Wachenfeldt K, Bentzon JF, Nielsen LB, Al-Mashhadi RH, Thygesen J, Tolbod L, Larsen JR, Frøkiær J, et al. Treatment with a human recombinant monoclonal IgG antibody against oxidized LDL in atherosclerosis-prone pigs reduces cathepsin S in coronary lesions. *Int J Cardiol*. 2016;215:506–515. doi: 10.1016/j.ijcard.2016.03.222
29. Badin JK, Bruning RS, Sturek M. Effect of metabolic syndrome and aging on Ca2+ dysfunction in coronary smooth muscle and coronary artery disease severity in Ossabaw miniature swine. *Exp Gerontol*. 2018;108:247–255. doi: 10.1016/j.exger.2018.04.024
30. Tharp DL, Masseau I, Ivey J, Laughlin MH, Bowles DK. Endurance exercise training does not limit coronary atherosclerosis in familial hypercholesterolemic swine. *Physiol Rep*. 2019;7:e14008. doi: 10.14814/phy2.14008
31. Glagov S, Weisenberg E, Zarins CK, Stankunavicius R, Kolettis GJ. Compensatory enlargement of human atherosclerotic coronary arteries. *N Engl J Med*. 1987;316:1371–1375. doi: 10.1056/NEJM198705283162204
32. Pedrigi RM, Poulsen CB, Mehta VV, Ramsing Holm N, Pareek N, Post AL, Kilic ID, Banya WA, Dall'Ara G, Mattesini A, et al. Inducing persistent flow disturbances accelerates atherogenesis and promotes thin cap fibroatheroma development in D374Y-PCSK9 hypercholesterolemic minipigs. *Circulation*. 2015;132:1003–1012. doi: 10.1161/CIRCULATIONAHA.115.016270
33. Koskinas KC, Chatzizisis YS, Papafaklis MI, Coskun AU, Baker AB, Jarolim P, Antoniadis A, Edelman ER, Stone PH, Feldman CL. Synergistic effect of local endothelial shear stress and systemic hypercholesterolemia on coronary atherosclerotic plaque progression and composition in pigs. *Int J Cardiol*. 2013;169:394–401. doi: 10.1016/j.ijcard.2013.10.021
34. Prescott MF, McBride CH, Hasler-Rapacz J, Von Linden J, Rapacz J. Development of complex atherosclerotic lesions in pigs with inherited hyper-LDL cholesterolemia bearing mutant alleles for apolipoprotein B. *Am J Pathol*. 1991;139:139–147.
35. Kolodgie FD, Gold HK, Burke AP, Fowler DR, Kruth HS, Weber DK, Farb A, Guerrero LJ, Hayase M, Kutys R, et al. Intraplaque hemorrhage and progression of coronary atheroma. *N Engl J Med*. 2003;349:2316–2325. doi: 10.1056/NEJMoa035655
36. Vieweg WV, Alpert JS, Johnson AD, Dennish GW, Nelson DP, Warren SE, Hagan AD. Distribution and severity of coronary artery disease in 500 patients with angina pectoris. *Cathet Cardiovasc Diagn*. 1979;5:319–330. doi: 10.1002/ccd.1810050404
37. Wadhera RK, Steen DL, Khan I, Giugliano RP, Foody JM. A review of low-density lipoprotein cholesterol, treatment strategies, and its impact on cardiovascular disease morbidity and mortality. *J Clin Lipidol*. 2016;10:472–489. doi: 10.1016/j.jacl.2015.11.010
38. Berneis KK, Krauss RM. Metabolic origins and clinical significance of LDL heterogeneity. *J Lipid Res*. 2002;43:1363–1379. doi: 10.1194/jlr.r200004-jlr200
39. Hoogeveen RC, Gaubatz JW, Sun W, Dodge RC, Crosby JR, Jiang J, Couper D, Virani SS, Kathiresan S, Boerwinkle E, et al. Small dense low-density lipoprotein-cholesterol concentrations predict risk for coronary heart disease: the Atherosclerosis Risk In Communities (ARIC) study. *Arterioscler Thromb Vasc Biol*. 2014;34:1069–1077. doi: 10.1161/ATVBAHA.114.303284
40. Kugiyama K, Doi H, Motoyama T, Soejima H, Misumi K, Kawano H, Nakagawa O, Yoshimura M, Ogawa H, Matsumura T, et al. Association of remnant lipoprotein levels with impairment of endothelium-dependent vasomotor function in human coronary arteries. *Circulation*. 1998;97:2519–2526. doi: 10.1161/01.cir.97.25.2519
41. Hoff HF, Morton RE. Lipoproteins containing apo B extracted from human aortas. Structure and function. *Ann N Y Acad Sci*. 1985;454:183–194. doi: 10.1111/j.1749-6632.1985.tb11857.x
42. Tabas I, Li Y, Brocia RW, Xu SW, Swenson TL, Williams KJ. Lipoprotein lipase and sphingomyelinase synergistically enhance the association of atherogenic lipoproteins with smooth muscle cells and extracellular matrix. A possible mechanism for low density lipoprotein and lipoprotein(a) retention and macrophage foam cell formation. *J Biol Chem*. 1993;268:20419–20432.
43. Schissel SL, Tweedie-Hardman J, Rapp JH, Graham G, Williams KJ, Tabas I. Rabbit aorta and human atherosclerotic lesions hydrolyze the sphingomyelin of retained low-density lipoprotein. Proposed role for arterial-wall sphingomyelinase in subendothelial retention and aggregation of atherogenic lipoproteins. *J Clin Invest*. 1996;98:1455–1464. doi: 10.1172/JCI118934
44. Oörni K, Hakala JK, Annila A, Ala-Korpela M, Kovanen PT. Sphingomyelinase induces aggregation and fusion, but phospholipase A2 only aggregation, of low density lipoprotein (LDL) particles. Two distinct mechanisms leading to increased binding strength of LDL to human aortic proteoglycans. *J Biol Chem*. 1998;273:29127–29134. doi: 10.1074/jbc.273.44.29127
45. Chatterjee SB, Dey S, Shi WY, Thomas K, Hutchins GM. Accumulation of glycosphingolipids in human atherosclerotic plaque and unaffected aorta tissues. *Glycobiology*. 1997;7:57–65. doi: 10.1093/glycob/7.1.57
46. Boyanovsky B, Karakashian A, King K, Giltiay N, Nikolova-Karakashian M. Uptake and metabolism of low density lipoproteins with elevated ceramide content by human microvascular endothelial cells: implications for the regulation of apoptosis. *J Biol Chem*. 2003;278:26992–26999. doi: 10.1074/jbc.M301536200
47. Edsfeldt A, Dunér P, Ståhlman M, Mollet IG, Asciutto G, Grufman H, Nitulescu M, Persson AF, Fisher RM, Melander O, et al. Sphingolipids contribute to human atherosclerotic plaque inflammation. *Arterioscler Thromb Vasc Biol*. 2016;36:1132–1140. doi: 10.1161/ATVBAHA.116.305675
48. Hartmann D, Wegner MS, Wanger RA, Ferreirós N, Schreiber Y, Lucks J, Schiffmann S, Geisslinger G, Grösch S. The equilibrium between long and very long chain ceramides is important for the fate of the cell and can be influenced by co-expression of CerS. *Int J Biochem Cell Biol*. 2013;45:1195–1203. doi: 10.1016/j.biocel.2013.03.012
49. Kleemann R, Verschuren L, van Erk MJ, Nikolsky Y, Cnubben NH, Verheij ER, Smilde AK, Hendriks HF, Zadelaar S, Smith GJ, et al. Atherosclerosis and liver inflammation induced by increased dietary cholesterol intake: a combined transcriptomics and metabolomics analysis. *Genome Biol*. 2007;8:R200. doi: 10.1186/gb-2007-8-9-r200
50. Jiang XC, Paultre F, Pearson TA, Reed RG, Francis CK, Lin M, Berglund L, Tall AR. Plasma sphingomyelin level as a risk factor for coronary artery disease. *Arterioscler Thromb Vasc Biol*. 2000;20:2614–2618. doi: 10.1161/01.atv.20.12.2614
51. Cheng JM, Suoniemi M, Kardys I, Vihervaara T, de Boer SP, Akkerhuis KM, Sysi-Aho M, Ekroos K, Garcia-Garcia HM, Oemrawsingh RM, et al. Plasma concentrations of molecular lipid species in relation to coronary plaque characteristics and cardiovascular outcome: results of the ATHEROREMO-IVUS study. *Atherosclerosis*. 2015;243:560–566. doi: 10.1016/j.atherosclerosis.2015.10.022
52. Havulinna AS, Sysi-Aho M, Hilvo M, Kauhanen D, Hurme R, Ekroos K, Salomaa V, Laaksonen R. Circulating ceramides predict cardiovascular outcomes in the population-based FINRISK 2002 cohort. *Arterioscler Thromb Vasc Biol*. 2016;36:2424–2430. doi: 10.1161/ATVBAHA.116.307497
53. Sharifi M, Rakhit RD, Humphries SE, Nair D. Cardiovascular risk stratification in familial hypercholesterolaemia. *Heart*. 2016;102:1003–1008. doi: 10.1136/heartjnl-2015-308845

Downloaded from http://ahajournals.org by on November 7, 2019